DMD Fast Forward. Published on July 17, 2018 as DOI: 10.1124/dmd.118.082545
This article has not been copyedited and formatted. The final version may differ from this version.

Metabolism of anethole dithiolethione by rat and human liver microsomes: formation of various products deriving from its O-demethylation and S-oxidation. Involvement of cytochromes P450 and flavin monooxygenases in these pathways.

Martin Dulac, Amor Sassi, Citra Nagarathinan, Marie-Odile Christen, Patrick Dansette, Daniel Mansuy, Jean-Luc Boucher

Laboratoire de Chimie et Biochimie Pharmacologiques et Toxicologiques, CNRS UMR 8601, University Paris Descartes, 45 rue des Saints-Pères, 75270 Paris, France (M.D., A.S., C.N., P.D., D.M., J-L.B.); Marie-Odile Christen Behavior, 27 rue Marceau 75116 Paris, France (M-O.C.)

Running title: Metabolism of anethole dithiolthione (Sulfarlem)

Correspondence to :

Jean-Luc Boucher, Laboratoire de Chimie et Biochimie Pharmacologiques et Toxicologiques, UMR 8601 CNRS, University Paris Descartes, 45 rue des Saints Pères, 75006 Paris, France.

Telephone : 33 (0)1 42 8621 91

Fax : 33 (0)1 42 86 83 87

Email: jean-luc.boucher@parisdescartes.fr

Text pages: 25

Tables: 2

Figures: 5

References: 35

Abstract: 137 words

Introduction: 478 words

Results and Discussion: 1284 words

Abbreviations

ADT, 5-(p-methoxyphenyl)-3H-1,2-dithiole-3-thione; ADO, 5-(p-methoxyphenyl)-3H-1,2-dithiole-3-one; ADTSO, 5-(p-methoxyphenyl)-3H-1,2-dithiole-3-thione sulfoxide; Bz-ImH, benzyl-imidazole; dmADT, 5-(p-hydroxyphenyl)-3H-1,2-dithiole-3-thione; dmADTSO, 5-(p-

hydroxyphenyl)-3H-1,2-dithiole-3-thione sulfoxide; dmADO, 5-(p-hydroxyphenyl)-3H-1,2-dithiole-3-one; CYP, cytochrome P450; DEXA, dexamethasone; FMO, flavin monoxygenase; HLM, human liver microsomes, HPLC-MS, high performance liquid chromatography-tandem mass spectrometry, β-NF, β-naphthoflavone; PB, Phenobarbital; PDA, photodiode array; pMA, 4-methoxy-acetophenone; pHA, 4-hydroxy-acetophenone; RLM, rat liver microsomes.

ABSTRACT

A study of the metabolism of anethole dithiolethione (ADT) by rat and human liver microsomes showed the formation of the corresponding S-oxide and the S-oxide of desmethyl-ADT (dmADT), and of p-methoxy-acetophenone (pMA) and p-hydroxy-acetophenone (pHA), in addition to the previously described metabolites, dmADT, anethole dithiolone (ADO) and its demethylated derivative, dmADO. The microsomal metabolism of ADO under identical conditions led to dmADO and to pMA and pHA. The metabolites of ADT derive from two competing oxidative pathways: an O-demethylation catalyzed by cytochromes P450 (CYPs) and an S-oxidation mainly catalyzed by flavin-dependent monooxygenases (FMOs) and, to a minor extent, by CYPs. The most active human CYPs for ADT demethylation appeared to be CYP1A1, 1A2, 1B1, 2C9, 2C19 and 2E1. ADT S-oxidation is catalyzed by FMOs 1 and 3, and, to a minor extent, by CYPs such as CYP3A4.

Introduction

Anethole dithiolethione (ADT, 5-(p-methoxyphenyl)-3H-1,2-dithiole-3-thione, formula in Figure 1) is a drug that has been marketed in many countries for many years and used in human therapy for its choleretic and sialogogic properties (Christen, 1995; Nagano et al., 2001). ADT also exhibits chemoprotective effects against cancer and various kinds of toxicity caused by some drugs and xenobiotics (Mansuy et al., 1986; Warnet et al., 1989; Reddy et al., 1993; Christen, 1995; Dollo et al., 1999; Lam et al. 2002; Kwak et al., 2003; Pouzaud et al., 2004; Zhang and Munday, 2008; Brooks et al., 2009). These chemoprotective effects appear to be mainly due to its antioxidant properties (Mansuy et al., 1986; Christen, 1995; Khanna et al., 1998) and its activity as a Nrf2 inducer, resulting in an increase of the GSH level and of the Phase II detoxifying enzymes (Lee and Surh, 2005; Giustarini et al., 2014).

ADT and its O-demethylated derivative, dmADT, were also extensively used as H_2S donors, and coupling of the OH group of dmADT with numerous anti-inflammatory drugs have led to a variety of compounds described for their H_2S-donor properties and their therapeutic effects (Chen et al., 2010; Sparatore et al., 2011; Kashfi and Olson, 2013; Couto et al., 2015). However, despite the use of ADT as a choleretic and sialologic drug for more than 50 years and the other promising protective and therapeutic effects of ADT and ADT linked to various drugs as H_2S donor hybrids, only few data have been published on the metabolism of ADT in mammals. It has been shown that it was O-demethylated to dmADT then conjugated into the corresponding glucuronide or sulfate *in vivo* in animals (rats, mice, rabbits and dogs) and humans (Gmelin and Lagler, 1963; Masoud and Bueding 1983; Sassi, 1986; Hayashi et al.,

1990). The formation of 5-(p-hydroxyphenyl)-3H-1,2-dithiole-3-one, ADO, and its O-demethylated derivative, dmADO (Figure 1) was also observed in rats and dogs (Hayashi et al., 1990). A more recent study of the metabolism of ADT by rat liver microsomes also showed the rapid formation of dmADT, and indicated the formation of metabolites resulting from the incorporation of an oxygen atom into ADT and dmADT. However the complete structure of those oxygenated metabolites was not determined (Chen et al., 2013).

The present article reports a study of the metabolism of ADT and ADO by human and rat liver microsomes and shows the formation of new metabolites, ADT and dmADT S-oxides (ADTSO and dmADTSO), p-methoxy-acetophenone (pMA) and p-hydroxy-acetophenone (pHA), in addition to dmADT, ADO and dmADO. It also shows that these metabolites derive from two competing oxidative pathways occurring on ADT: an O-demethylation catalyzed by cytochromes P450 (CYPs) and an S-oxidation catalyzed by flavin-dependent monooxygenases (FMOs) and CYPs. Finally, a study of the oxidation of ADT by recombinant human liver microsomal CYPs and FMOs allowed one to compare the abilities of those enzymes to catalyze ADT oxidation.

MATERIALS and METHODS

General reagents

ADT was purchased from APIChem Technology (Hangzhou, Zhejiang, PR China). NADPH, NADP, G6P, G6PDH, miconazole, N-benzyl-imidazole (Bz-ImH), pHA, pMA, and all other chemicals were purchased from Sigma-Aldrich (Saint-Quentin Fallavier, France) and were of the highest commercially available purity. HPLC-grade acetonitrile and methanol were obtained from SDS (Peypin, France).

Synthesis of authentic samples

DmADT was prepared by heating ADT in the presence of pyridine hydrochloride for 30 min at 215°C, as previously described (Chen et al., 2010). ADO and dmADO were prepared by treatment of ADT and dmADT, respectively, in the presence of mercuric acetate as previously described (Klingsberg, 1972). ADTSO and dmADTSO were prepared from ADT and dmADT, respectively, by treatment with 3-chloroperbenzoïc acid at 0°C for 1h in dichloromethane, as previously described (Perez and Kresze, 1981; Biart et al., 1992). All derivatives displayed ^{1}H NMR (Supporting Information Table S1), UV-visible (Supporting Information Table S2) and high resolution mass spectra (Supporting Information Figure S1) in accordance with their structures.

Origin of microsomes and recombinant enzymes

Rat liver microsomes (RLM) were prepared as previously reported (Kremers et al., 1981) from male Sprague-Dawley rats (Charles River, L'Arbresle, France) treated either with phenobarbital (PB) (20 mg.kg^{-1}, in 0.9% NaCl, i.p. for 4 days), β-naphthoflavone

(β-NF) or dexamethasone (DEXA) (each 50 $mg.kg^{-1}$, in corn oil, i.p. for 4 days). Recombinant CYP1A1, 1A2, 1B1, 2A6, 2C9, 2C19, 2D6, 2E1 and 3A4, co-expressed in baculovirus-transfected insect cells with human cytochrome P450 oxido-reductase and cytochrome b5 (Supersomes) were from Corning Inc (Corning, Amsterdam, The Netherlands). Human liver microsomes (HLM) and recombinant FMO1 and FMO3 were also from Corning Inc. Protein concentrations were determined by the Bradford assay with bovine serum albumin as a standard (Bradford, 1976). Cytochrome P450 contents were determined by the method of Omura and Sato (Omura and Sato, 1964).

Typical microsomal incubation procedures

The standard oxidation reactions were conducted in 50 mM potassium phosphate buffer (pH 7.4) containing 0.1 mM EDTA, microsomal proteins (usual concentration 3 μM CYP), and 0.1 mM substrate. The mixtures were incubated for 2 min at 37°C and the reactions (final volumes 200 μL) were started by the addition of NADPH (1 mM) and a NADPH regenerating system (0.5 mM NADP + 5 mM G6P + 1 U/mL G6PDH). Usual incubations were carried out for 0-120 min at 37°C and were quenched by the addition of 100 μl of a cold acetonitrile-acetic acid (10:1 v/v) mixture. Reaction mixtures were centrifuged (10 000 g, 10 min) to sediment the precipitated proteins and aliquots of the supernatants were injected onto the HPLC-MS system. Incubations of ADT and ADO with recombinant CYPs or FMOs were performed under identical conditions except that the incubation mixtures contained 20 pmol of recombinant CYP or 0.2 mg/mL FMO. Control experiments were carried out under identical conditions but without protein or without NADPH and NADPH regenerating system.

Large scale (100 mL) incubations of ADT in the presence of liver microsomes from PB-pretreated rats were performed as above and were extracted with ethyl acetate. After evaporation of solvent, ADT and its metabolites were separated on a Hypersil C18 column (250 x 3/8", 5 µm; SFCC, Eragny, France). Elution was performed under isocratic condition using a mixture of water-methanol-acetic acid (60/40/1, v/v) at a flow rate of 3 mL/min and UV detection was performed at 310 nm.

HPLC-MS-MS analyses of metabolites

The supernatants were analyzed on a Surveyor HPLC system including a PDA detector and coupled to a LCQ Advantage ion trap mass spectrometer (Thermo, Les Ulis, France). HPLC separations were achieved on a Gemini C18 column (100 x 2 mm, 3 µm; Phenomenex, Le Pecq, France). Elution (flow rate 250 µL/min) was performed using a mixture of solvent A (water + 0.1% formic acid) and B (acetonitrile + 0.1% formic acid) with the following gradient conditions: 10% B for 1 min, linear gradient to 80% B in 18 min, linear gradient to 100% B in 1 min, holding at 100% B for 3 min, returning to 10 % B in 0.1 min, and re-equilibration at 10% B for 5 min. The column effluent was directed to the ion source from 3 to 23 min after injection to reduce contamination. Mass spectra were obtained by electrospray ionisation in the positive detection mode under the following conditions: source parameters: capillary temperature, 250°C; capillary voltage, 6 V; spray voltage, 4.5 kV; primary gas flow, 20 a.u.; auxillary gas flow, 5 a.u. Mass spectra were recorded with a resolution of 1 a.m.u., with a frequency of 50 ms. The range of masses scanned for the total-ion chromatogram was *m/z* 120-600. For all products, the indicated molecular ions corresponded to $M+H^+$ (i.e. ADT, *m/z* 241, ADO, *m/z* 225). After data acquisition, HPLC-MS chromatograms

and UV-Vis spectra (230-550 nm) were analyzed with Excalibur LC Device 2.2.0 software (Thermo). Quantitation of ADT and of its metabolites was performed by integration of UV-visible spectra using calibration curves obtained from incubations of authentic compounds incubated, worked-up and analyzed in an identical fashion to that described above, except that NADPH and the NADPH-regenerating system were omitted.

DMD Fast Forward. Published on July 17, 2018 as DOI: 10.1124/dmd.118.082545
This article has not been copyedited and formatted. The final version may differ from this version.

RESULTS and DISCUSSION

Metabolism of ADT by rat and human liver microsomes

The HPLC-MS chromatogram of incubates of 100 µM ADT with liver microsomes from rats pretreated with β-NF in the presence of an NADPH generating system (Figure 2) showed the formation of the previously described metabolites (Gmelin and Lagler, 1963; Masoud and Bueding, 1983; Hayashi et al., 1990; Chen et al., 2013): dmADT as a major metabolite and ADO and dmADO in smaller amounts. It also showed the formation of four other metabolites: ADTSO and dmADTSO, resulting from an S-oxidation of the C=S moiety of ADT and dmADT, respectively, and pMA and pHA, two compounds resulting from the cleavage of the dithiolthione ring with loss of a carbon atom. All these metabolites were obtained from semi-preparative HPLC and completely identified by comparison of their HPLC retention times, UV-visible, MS and ^{1}H NMR spectra with those of authentic samples that were synthesized as indicated in Materials and Methods or commercially obtained in the case of pMA and pHA. It is likely that the S-oxide ADTSO is the oxygenated metabolite of ADT mentioned by Chen *et al.* (Chen et al., 2013). Figure 3A shows a typical kinetic study of the metabolism of ADT in the presence of liver microsomes from rats pretreated with β-NF. First, ADT was predominantly metabolized into dmADT and small amounts of ADTSO, ADO, dmADO and pMA. DmADT, ADTSO and ADO then decreased with a concomitant increase in dmADO and pMA formation. Identical incubations of ADT but in the absence of microsomes or NADPH did not lead to any formation of those metabolites (data not shown). Table 1 compares the amounts of the ADT metabolites formed upon 2 h incubations of ADT with a NADPH regenerating system and liver

microsomes from rats pretreated by several inducing agents, β-NF, PB, or DEXA, or with HLM. It shows that the same metabolites are formed with the three types of RLM. However, it is noteworthy that liver microsomes from DEXA-pretreated rat are less active for ADT oxidation (25% residual ADT instead of 6-7% in the case of β-NF- or PB-treated rats after 2 h). Moreover, they led to much less metabolites derived from an ADT O-demethylation (22% compared to 75% total metabolites instead of about 60% compared to 94% total metabolites in the case of the two other RLM) (Table 1). HLM predominantly catalyzed the O-demethylation of ADT (65% of all metabolites), but with a lower activity than the β-NF and PB-pretreated RLM (30% residual ADT after 2 h) (Table 1). Interestingly, incubation of ADT with liver microsomes from β-NF-treated rats in the presence of a NADPH-regenerating system and of 5 mM glutathione almost exclusively led to dmADT (Figure 3B). Identical results were observed with HLM (data not shown). The lack of formation of ADTSO and metabolites deriving from ADTSO, such as ADO and pMA, in the presence of GSH could be explained by the reduction of the sulfoxide function of ADTSO by GSH back to ADT. Actually, reaction of 100 µM ADTSO with 1mM GSH in 50 mM potassium phosphate buffer (pH 7.4) containing 0.1 mM EDTA for 30 min at 37°C almost quantitatively led to ADT. In a similar manner, reaction of dmADTSO with GSH under identical conditions almost exclusively led to dmADT (data not shown).

Metabolism of ADO by liver microsomes

To assess the sequential metabolism of ADT, incubations were conducted using ADO as the starting compound. Metabolism of ADO by rat or human liver microsomes under conditions identical to those used previously for ADT led to the three metabolites

already observed in the case of ADT, dmADO, pMA and pHA. Figure 4 shows the kinetics of formation of those metabolites in incubations of ADO with β-NF-treated rat liver microsomes and HLM (Figure 4A and 4B, respectively). These data showed that pMA is a metabolite of ADO and suggested that pHA derives from dmADO. Accordingly, incubation of dmADO with the same microsomes led to pHA as a major metabolite (data not shown).

The above data about ADT and ADO microsomal metabolism indicated that ADT metabolites derive from two pathways for oxidation of the molecule: an O-demethylation and an S-oxidation leading respectively to dmADT and ADTSO as primary metabolites (Figure 5). ADTSO should then lead to ADO by oxidative desulfuration in a manner similar to what was reported for the oxidative desulfuration of compounds containing a C=S moiety (Hanzlik and Cashman, 1983) and to pMA deriving from ADO as shown in Figure 5. The further microsomal metabolism of the other primary metabolite dmADT should be similar to that of ADT, with the formation of metabolites deriving from an S-oxidation, dmADTSO, dmADO and pHA (Figure 5). Accordingly, metabolism of dmADT with the same microsomes led to dmADTSO, dmADO and pHA as major metabolites (data not shown).

Nature of the microsomal enzymes involved in the metabolism of ADT

In order to determine the enzymes involved in the human liver metabolism of the drug ADT, incubations of ADT with several recombinant human CYPs and FMOs involved in xenobiotics metabolism were performed. Table 2 shows that CYPs of family 1 (CYP1A1, 1A2 and 1B1) and CYP2C19 are very good catalysts for ADT oxidation (O-demethylation + S-oxidation). CYP2C9, 2D6, 2E1, and 3A4 are also active for ADT

oxidation, even though less than those of family 1, whereas CYP2A6 is much less active. Moreover, the observed O-demethylation/S-oxidation ratio very much varied as a function of the involved CYPs. This ratio was much in favor of O-demethylation in the case of CYP1B1, 2C19, 1A2, 2C9, 1A1, and 2E1 (values from 25 to 4), whereas it was in favor of S-oxidation for CYP2D6 and 3A4 (values of about 0.5 and close to 0, respectively). Interestingly, recombinant FMOs 1 and 3 failed to catalyze ADT O-demethylation, as expected (Cashman, 1995; Cashman and Zhang, 2006), but were active for ADT S-oxidation (Table 2). Actually, inactivation of microsomal FMOs by preheating of HLM at 45°C for 10 min (Cashman and Zhang, 2006) led to a 60% decrease of the formation of ADTSO and ADO whereas it led to an increase of the formation of the O-demethylated product dmADT (data not shown). Moreover, incubation of ADT with HLM in the presence of an usual CYP inhibitor, N-benzyl-imidazole (1mM) (Testa and Jenner, 1981; Correia and Ortiz de Montellano, 2005), led to a 60% inhibition of dmADT formation and only led to a 20% decrease of the ADTSO formation (data not shown). These data indicated that ADT S-oxidation was mainly catalyzed by FMOs and to a minor extent by CYPs. The results of Table 2 also show that ADO was formed upon oxidation of ADT by most recombinant human CYPs and FMOs, indicating that both enzymes are also able to catalyze the oxidation of ADTSO to ADO. We have confirmed this point in the particular case of recombinant CYP3A4. Actually, incubations of 100 μM ADTSO for 1 h at 37°C in the presence of 0.2 μM recombinant CYP3A4 and 1 mM NADPH led to ADO as the major product (data not shown).

The above data indicate that the products formed upon metabolism of ADT by HLM derive from two pathways, an oxidative CYP-catalyzed O-demethylation (CYPs of

family 1 and CYP2C19, 2C9 and 2E1 being the most active ones) and an S-oxidation of the C=S group of ADT catalyzed by FMOs and by some CYPs such as CYP3A4. This should also be true for ADT metabolism by RLM as the greatest O-demethylation/S-oxidation ratio was observed in the case of microsomes of rats pretreated with β-NF, an inducer of P450s from family 1, the lowest O-demethylation/S-oxidation ratio being observed in the case of microsomes of rats pretreated with DEXA, an usual inducer of P450s from the 3A subfamily (Williams et al., 2005).

CONCLUSION

The above described reinvestigation of ADT metabolism and study of ADO metabolism by rat and human liver microsomes clearly established the formation of new metabolites, ADTSO, dmADTSO, pMA and pHA, in addition to the previously described metabolites, dmADT, ADO and dmADO (Gmelin and Lagler; 1963; Hayashi et al., 1990; Chen et al., 2013). They also showed that all these metabolites derive from two primary pathways, a CYP-dependent O-demethylation of ADT, and an S-oxidation of the C=S group of ADT that is catalyzed both by FMOs and CYPs. The use of recombinant human P450s showed that CYPs of family 1 and CYP2C19, 2C9, and 2E1 are the most active ones for ADT O-demethylation. ADO and the opened products having lost one carbon and the three sulfur atoms of ADT, pMA and pHA, are derived from the ADT S-oxidation pathway that can be catalyzed by FMOs and some CYPs

such as CYP3A4. The reactions involved in the passage from ADO to pMA are under study.

Acknowledgments

The authors thank A. Hessani for her help in HPLC-MS experiments, and M. Jaouen and B. Ramassamy for their technical assistance.

Authorship contributions

Participated in research design: Dansette, Boucher, Mansuy, Christen.

Conducted experiments: Dulac, Sassi, Nagarathinan, Boucher.

Contributed new reagents or analysis tools: Dulac, Sassi, Boucher, Dansette.

Performed data analysis: Dulac, Sassi, Boucher, Dansette, Mansuy.

Wrote or contributing to the writing of the manuscript: Mansuy, Boucher, Dansette.

References

Biard D, Christen MO, Dansette P, Jasserand D, Mansuy D, and Sassi A (1992) 1,2-Dithiol-3-thion-S-oxide compounds and pharmaceutical compositions. US Patent 5,096,920.

Bradford MM (1976) A rapid and sensitive method for the quantitation of microgram quantities of protein utilizing the principle of protein-dye binding. *Anal Biochem* **72**: 248-254.

Brooks SC, Brooks JS, Lee WH, Lee MG, and Kim SG (2009) Therapeutic potential of dithiolethiones for hepatic diseases. *Pharmacol Ther* **124**:31-43.

Cashman JR and Zhang J (2006) Human flavin-containing monoxygenases. *Annu Rev Pharmacol Toxicol* **46**:65-100.

Cashman JR (1995) Structural and catalytic properties of mammalian flavin-containing monooxygenase. *Chem Res Toxicol* **8**:165-181.

Chen MH, Liu MH, Di B, and Su MX (2013) Anethol trithione metabolites and their mutual transformation. *Chinese J New Drugs* **22**:2328-2331.

Chen P, Luo Y, Hai L, Qian S, and Wu Y (2010) Design, synthesis, and pharmacological evaluation of the aqueous prodrugs of desmethyl anethole trithione with hepatoprotective activity. *Eur J Med Chem* **45**:3005-3010.

Christen MO (1995) Anethole dithiolethione: Biochemical considerations, *Methods Enzymol* **252**:316-323.

Correia MA, and Ortiz de Montellano PR (2005) Inhibition of Cytochromes P450 enzymes, in *Cytochrome P450, Structure, mechanism, and Biochemistry* 3rd Edition (Ortiz de Montellano PR ed) pp 247-322, Kluwer Academic/Plenum Publishers, New York.

Couto M, de Ovalle S, Cabrera M, Cerecetto H, González M (2015) Searching phase II enzymes inducers, from Michael acceptor-[1,2]dithiolethione hybrids, as cancer chemopreventive agents. *Future Med Chem* **7**:857-871.

Dollo G, Le Corre P, Chollet M, Chevanne F, Bertault M, Burgot JL, and Le Verge R (1999) Improvement in solubility and dissolution rate of 1, 2-dithiole-3-thiones upon complexation with beta-cyclodextrin and its hydroxypropyl and sulfobutyl ether-7 derivatives. *J Pharm Sci* **88**:889-895.

Giustarini D, Fanti P, Sparatore A, Matteucci E, and Rossi R (2014) Anethole dithiolethione lowers the homocysteine and raises the glutathione levels in solid tissues and plasma of rats: a novel non-vitamin homocysteine-lowering agent. *Biochem Pharmacol* **89**:246-254.

Gmelin R, and Lagler F (1963) Tolerance and excretion of anetholtrithion, *Arzneimittelforschung* **13**:130-133.

Hayashi T, Okuyama Y, Komura H, Morino A, Sugiyama M, and Nomura A (1990) Studies on the metabolic fate of anethole trithione. *Iyakuhin Kenkyu* **21**: 584–602.

Hanzlik RP, and Cashman JR (1983) Microsomal metabolism of thiobenzamide and thiobenzamide S-oxide. *Drug Metab Dispos* **11**:201-205.

Khanna S, Sen CK, Roy S, Christen MO, and Packer L (1998) Protective effects of anethole dithiolethione against oxidative stress-induced cytotoxicity in human Jurkat T cells. *Biochem Pharmacol* **56**:61-69.

Kashfi K, and Olson KR (2013) Biology and therapeutic potential of hydrogen sulfide and hydrogen sulfide-releasing chimeras. *Biochem Pharmacol* **85**:689-703.

Klingsberg E (1972) The 1,2-Dithiolium Cation. XI. Polycyclic dithiole and "No-Bond resonance compounds. *J Org Chem* **57**:3226-3229.

Kremers P, Beaune P, Cresteil T, de Graeve J, Columelli S, Leroux JP, and Gielen JE (1981) Cytochrome P-450 monooxygenase activities in human and rat liver microsomes. *Eur J Biochem* **118**: 599−606.

Kwak MK, Wakabayashi N, Itoh K, Motohashi H, Yamamoto M, and Kensler TW (2003) Modulation of gene expression by cancer chemopreventive dithiolethiones through the Keap1-Nrf2 pathway. Identification of novel gene clusters for cell survival. *J Biol Chem* **278**:8135-8145.

Lam S, MacAulay C, Le Riche JC, Dyachkova Y, Coldman A, Guillaud M, Hawk E, Christen MO, and Gazdar AF (2002) A randomized phase IIb trial of anethole dithiolethione in smokers with bronchial dysplasia. *J Natl Cancer Inst* **94**:1001-1009.

Lee JS, and Surh YJ (2005) Nrf2 as a novel molecular target for chemoprevention. *Cancer Lett* **224**:171-184.

Mansuy D, Sassi A, Dansette PM, and Plat M (1986) A new potent inhibitor of lipid peroxidation *in vitro* and *in vivo*, the hepatoprotective drug anisyldithiolthione. *Biochem Biophys Res Commun* **135**:1015-1021.

Masoud AN, and Bueding E (1983) Identification and quantitation of a metabolite of anethol dithiolthione in rat and mouse urine using high-performance liquid chromatography. *J Chromatogr* **276**:111-119.

Nagano T, and Takeyama M (2001) Enhancement of salivary secretion and neuropeptide (substance P, α-calcitonin gene-related peptide) levels in saliva by chronic anethole trithione treatment. *J Pharm Phamacol* **53**:1697-1702.

Omura T, and Sato R (1964) The carbon monoxide-binding pigment of liver microsomes. Evidence for its hemoprotein nature. *J Biol Chem* **239**: 2370-2378.

Perez MA, and Kresze G (1981) 3*H*-1,2-Dithiol-3-thion-*S*-oxide. *Liebigs Ann Chem* 1510-1512.

Pouzaud F, Christen MO, Warnet JM, and Rat P (2004) Anethole dithiolethione: an antioxidant agent against tenotoxicity induced by fluoroquinolones. *Pathol Biol (Paris)* **52**:308-313.

Reddy BS, Rao, CV, Rivenson A, and Kelloff G (1993) Chemoprevention of colon carcinogenesis by organosulfur compounds. *Cancer Res* **53**:3493-3498.

Sassi A (1986) PhD thesis, University Paris-Sud. Metabolisme et origine des effets hepatoprotecteurs des dérives de l'anisyldithiolethione.

Sparatore A, Santus G, Giustarini D, Rossi R, and Del Soldato P (2011) Therapeutic potential of new hydrogen sulfide-releasing hybrids. *Expert Rev Clin Pharmacol* **4**:109-121.

Testa B, and Jenner P (1981) Inhibitors of Cytochrome P-450s and their mechanism of action. *Drug Metab Rev* **12**:1-117.

Warnet JM, Christen MO, Thevenin M, Biard D, Jacqueson A, and Claude JR (1989) Protective effect of anethol dithiolthione against acetaminophen hepatotoxicity in mice. *Pharmacol Toxicol* **65**:63-64.

Williams SN, Dunham E, and Bradfield CA (2005) Induction of cytochrome P450 enzymes, in *Cytochrome P450, Structure, mechanism, and Biochemistry* 3rd Edition (Ortiz de Montellano PR ed) pp 323-346, Kluwer Academic/Plenum Publishers, New York.

Zhang Y, and Munday R (2008) Dithiolethiones for cancer chemoprevention: where do we stand? *Mol Cancer Ther* **7**:3470-3479.

FIGURE LEGENDS

Figure 1: Formula of ADT and some of its metabolites.

Figure 2: HPLC chromatogram with PDA-detection from representative 2h incubation at 37°C of 100 μM ADT with liver microsomes from β-NF-pretreated rats (3.0 μM P450) in the presence of a NADPH-generating system. The incubation was conducted, treated and analyzed by HPLC-MS as described in Materials and Methods. The little blue squares appearing along the baseline are integration points.

Figure 3: (A) Representative kinetics of ADT metabolism by liver microsomes from β-NF-pretreated rats (3.0 μM P450) under conditions indicated in Materials and Methods. (B) Kinetics of an identical incubation containing 5 mM GSH. ADT, black squares; dmADT, red empty triangles; dmADO, blue diamonds; ADTSO, red filled triangles; ADO, blue filled circles; pMA, green empty circles.

Figure 4: Kinetics of ADO metabolism by liver microsomes from β-NF-pretreated rats (3.0 μM P450) (A) or by HLM (2.2 μM P450) (B). Conditions indicated in Materials and Methods. ADO, black squares; dmADO, red triangles; pMA, blue circles; pHA, green diamonds.

Figure 5: Reactions involved in the metabolism of ADT and ADO by HLM and RLM.

Table 1. Metabolism of ADT by liver microsomes from rats pretreated with different inducing agents and by HLM[a].

Compounds	% Total metabolites [b]			
	β-NF	**PB**	**DEXA**	**HLM**
ADT	7 ± 2	6 ± 2	25 ± 4	30 ± 5
dmADT	53 ± 5	45 ± 4	12 ± 3	46 ± 5
ADTSO	4 ± 2	9 ± 2	18 ± 3	5 ± 2
ADO	4 ± 1	2 ± 1	15 ± 3	5 ± 3
dmADTSO	3 ± 2	4 ± 2	4 ± 2	n.d. [c]
dmADO	11 ± 1	6 ± 2	6 ± 2	n.d. [c]
pMA	16 ± 2	25 ± 3	18 ± 2	12 ± 3

[a] The amounts of pHA were too low to be accurately quantified. [b] Data are expressed as % metabolites formed after 2 h incubation of 100 μM ADT in the presence of β-NF-, PB- and DEXA-pretreated rat liver microsomes, or HLM, as indicated in Materials and Methods. Data are means ± s.d. from 2-5 experiments. [c] Not detected.

DMD Fast Forward. Published on July 17, 2018 as DOI: 10.1124/dmd.118.082545
This article has not been copyedited and formatted. The final version may differ from this version.

Table 2. Metabolism of ADT with microsomes from insect cells expressing various recombinant human CYPs and FMOs (Supersomes)[a].

	ADT	**dmADT**	**ADTSO**	**ADO**	**dmADO**	**pMA**
CYP1A1	36 ± 2	58 ± 5	n.d.[b]	8 ± 2	2 ± 1	1 ± 1
CYP1A2	18 ± 2	75 ± 5	n.d.	3 ± 2	4 ± 2	1 ± 1
CYP1B1	22 ± 4	74 ± 5	n.d.	3 ± 2	1 ± 1	n.d.
CYP2A6	93 ± 6	n.d.	n.d.	6 ± 2	n.d.	n.d.
CYP2C9	73 ± 6	23 ± 4	n.d.	3 ± 2	1 ± 1	n.d.
CYP2C19	21 ± 4	75 ± 6	n.d.	3 ± 1	1 ± 1	n.d.
CYP2D6	48 ± 5	16 ± 4	n.d.	28 ± 4	n.d.	6 ± 2
CYP2E1	44 ± 5	35 ± 5	n.d.	7 ± 2	8 ± 3	4 ± 2
CYP3A4	47 ± 5	n.d.	n.d.	40 ± 5	n.d.	13 ± 4
FMO1	72 ± 6	n.d.	4 ± 2	16 ± 4	n.d.	6 ± 2
FMO3	93 ± 5	n.d.	4 ± 2	3 ± 1	n.d.	n.d.

[a] % ADT or metabolite yields ± s. d. from 2-4 experiments, from 100 μM ADT after 2 h incubation in the presence of 0.2 μM recombinant CYPs or from 1 h incubations containing 1 mg/mL recombinant FMOs. Quantitation of ADT and of its metabolites was performed by integration of UV-visible spectra using calibration curves as described in Materials and Methods. [b] Not detected

DMD Fast Forward. Published on July 17, 2018 as DOI: 10.1124/dmd.118.082545
This article has not been copyedited and formatted. The final version may differ from this version.

Figure 1

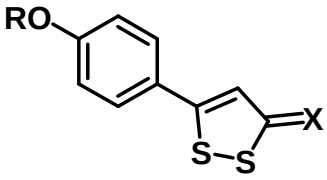

ADT	**X = S**	**R = CH_3**
dmADT	**X = S**	**R = H**
ADTSO	**X = SO**	**R = CH_3**
dmADTSO	**X = SO**	**R = H**
ADO	**X = O**	**R = CH_3**
dmADO	**X = O**	**R = H**

DMD Fast Forward. Published on July 17, 2018 as DOI: 10.1124/dmd.118.082545
This article has not been copyedited and formatted. The final version may differ from this version.

Figure 2

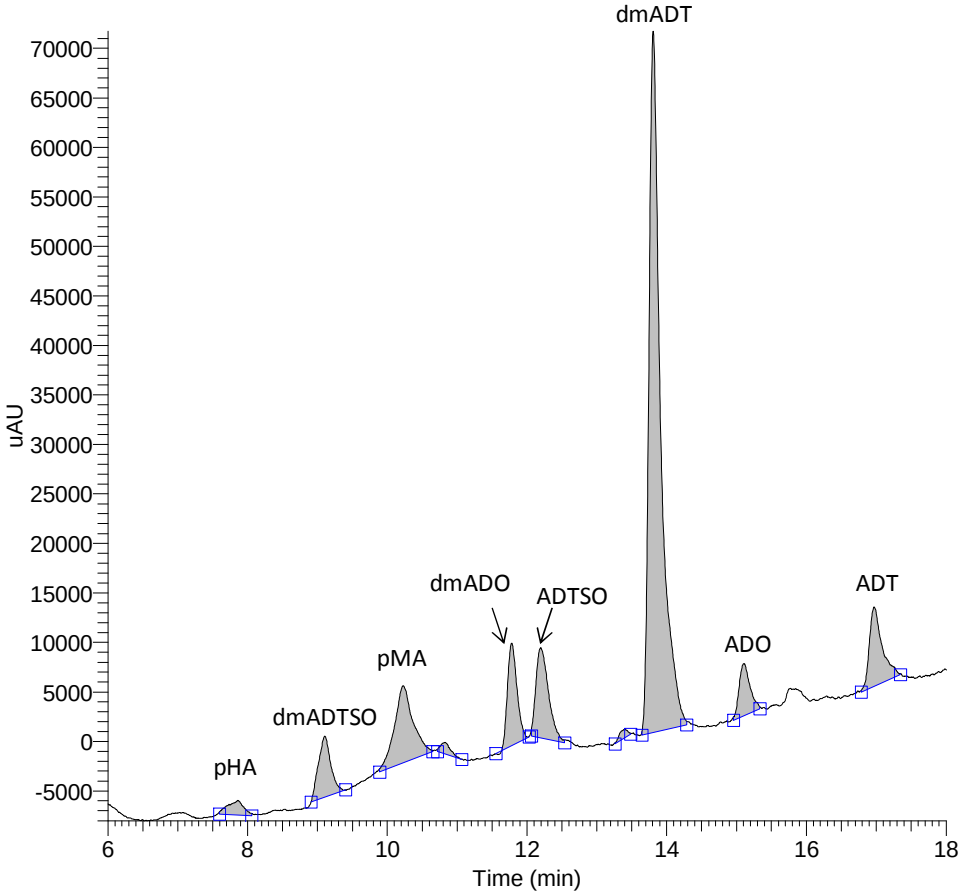

DMD Fast Forward. Published on July 17, 2018 as DOI: 10.1124/dmd.118.082545
This article has not been copyedited and formatted. The final version may differ from this version.

Figure 3

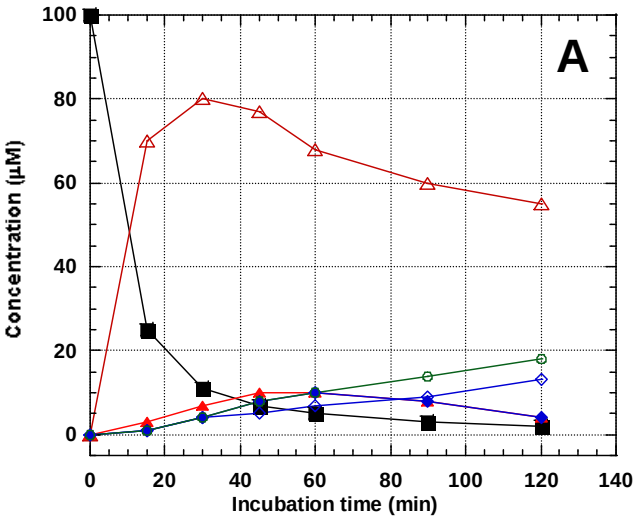

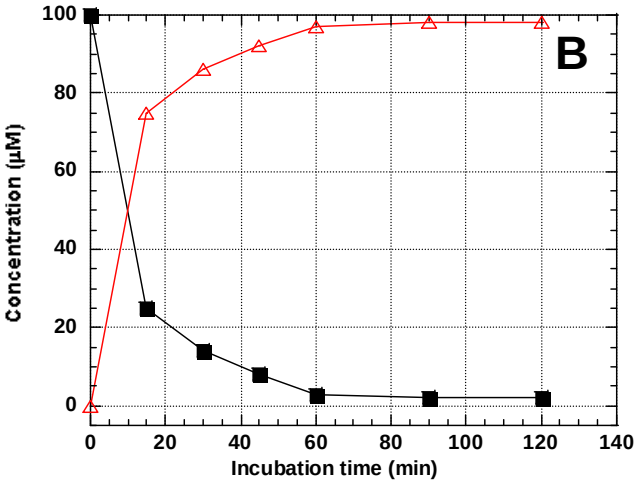

DMD Fast Forward. Published on July 17, 2018 as DOI: 10.1124/dmd.118.082545
This article has not been copyedited and formatted. The final version may differ from this version.

Figure 4

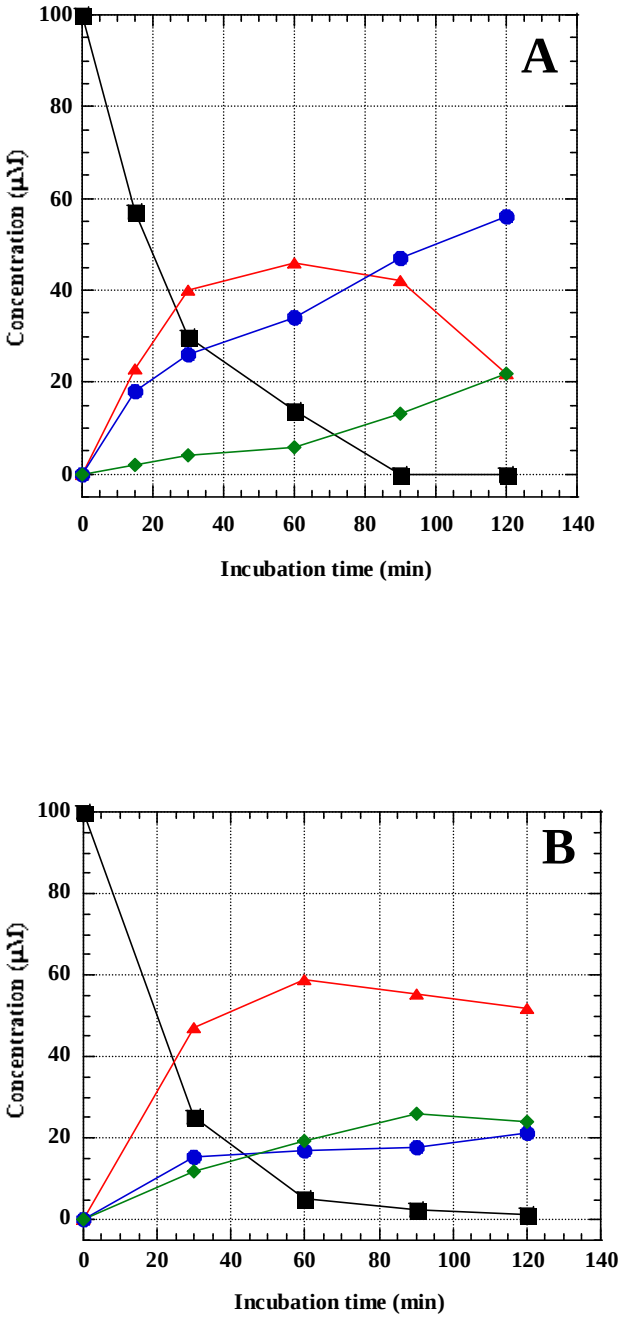

DMD Fast Forward. Published on July 17, 2018 as DOI: 10.1124/dmd.118.082545
This article has not been copyedited and formatted. The final version may differ from this version.

Figure 5